



Article Processing Dates: Received on 2024-01-09, Reviewed on 2024-01-22, Revised on 2024-02-02, Accepted on 2024-02-21 and Available online on 2024-02-29

Enhancing TIG Welding Parameters For Direct Tensile Load (DT-load) On Various Steel Thicknesses

Amar¹, Arul Basit¹, Tegar Dwi Cahyo¹, Sukarman^{1*}, Khoirudin¹, Dodi Mulyadi¹, Ade Suhara², Apang Djafar Shiedique³

¹Department of Mechanical Engineering, Universitas Buana Perjuangan Karawang, Karawang, 14640, Indonesia

²Department of Industrial Engineering, Universitas Buana Perjuangan Karawang, Karawang, 14640, Indonesia

³Department of Mechanical Engineering, Sekolah Tinggi Teknologi Wastukencana, Purwakarta, 14640, Indonesia

*Corresponding author: sukarman@ubpkarawang.ac.id

Abstract

The car-body repair process is integral to vehicle development and structural repair. The primary objective of this study was to enhance the quality of thin material welding utilised in automobile body repair. The impetus for this research stems from the necessity to improve the structural integrity and longevity of thin materials prone to deformation throughout the welding procedure while minimizing distortion. This study aims to identify the optimal parameters for Tungsten Inert Gas welding (TIG welding) on thin materials, particularly for automobile body rearrangement. The Taguchi method was used to conduct an experimental analysis of variations in welding parameters, including the electrode diameter, gas flow rate, and welding current. According to the findings of this study, adjusting TIG welding parameters to their optimal values significantly improves the weld joint Direct Tensile load (DT-load) and overall structural quality. ANOVA analysis and the S-N ratio indicate that gas flow rate and welding current are significant determinants of the quality of welded joints in thin materials. This research contributes to a better understanding of the optimal parameters for fusing thin materials, particularly in automobile body repair. The automotive industry can use these findings as a guide to enhance the quality and strength of welding processes, which are critical to the structural integrity of vehicles.

Keywords:

Direct tensile load, TIG welding, automobile body repair, gas flow rate, Taguchi method.

1 Introduction

Thin materials are commonly joined using Resistance Spot Welding (RWS) to fabricate vehicle body components, such as the frame or interior[1]. Owing to its limited feasibility, Resistance Spot Welding (RSW) is not commonly used in body-repair workshops. To ensure the structural integrity and operational efficiency of a vehicle, it is essential to distribute the tensile load uniformly across critical areas when performing welding repair. TIG welding is often employed as an effective method to repair automobile bodies. To improve the reliability and durability of TIG-welded joints, it is crucial to optimize welding process parameters. This involves achieving maximum tensile strength while maintaining the safety and functionality of the vehicle.

In total, there were approximately 34, 500 and 33,000 workshops of car body repair companies based on the 2008 and 2022 data, respectively [2, 3]. Despite Indonesia's abundant auto body repair shops, more precise statistical data on the past five years must be collected. In 2013, Indonesia had an estimated 1,130 workshops on automotive body repair[6]. Fig. 1 shows the welding process at the Mercedes-Benz workshop [5].

TIG welding utilizes argon, helium, and tungsten electrodes to shield the welding area [7]. TIG welding is extensively used owing to its numerous advantages, including excellent safety features, a stable electric arc, easy regulation of the heat input, minimal material sintering, and the ability to achieve a high-quality welding appearance [8]. Nevertheless, it is important to acknowledge that TIG welding has certain disadvantages such as limited penetration depth and reduced efficiency [9]. This limitation hinders the TIG welding implementation, leading to higher production costs [8]. The SPCC-SD steel sheet is distinguished by its chemical composition, which features a relatively low carbon content ranging from 0.05 to 0.25 percent by weight [9]. The thickness of automobile body low-carbon steel typically ranges from 0.6 to 0.98 mm [10].

The previously studied TIG welding used St 37, SUS 316 L, and AA6061. In this study, Tungsten Inert Gas (TIG) welding was employed to assess the impact of filler size and electric current on the microstructure and tensile strength of St 37, a low-carbon steel[6]. A series of tensile tests was performed on a welded joint, revealing a maximum tensile strength of 41.74 N/mm². The outcomes were achieved and completed through TIG welding utilizing an electric current and a 1.6 mm filler size. Conversely, when a welding current of 120 A and filler diameter of 2.0 mm were used, the resulting tensile strength was the lowest at 39.71 N/mm². Budiyanto et al. [10] conducted further investigation and documented the use of TIG welding on SUS 316L material, with varying welding speed and current as input parameters. Data collection encompassed essential factors, including the microstructure and hardness of the material. The findings suggest a positive correlation between the size of the electric current and the microstructure of the grains, and the welding rate is negatively correlated with the previously mentioned factor. This paradox can be explained by the observation that larger microstructure grains decrease welding speed. The weld metal and the Heat-Affected Zone (HAZ) exhibited the highest hardness levels in the material. The hardness values varied from the lowest to the highest along the base metal. The most challenging conditions were a TIG welding speed of 12 cm/min and current of 100 A.

Further investigation into the utilization of AA6061 alloy in TIG welding was reported by [11]. The investigation utilized three welding variables across four experimental levels, in combination with the Taguchi methodology. The input parameters of the study included the velocity, gas flow rate, and welding current. The enquiry primarily focused on carefully chosen and calculated values of impact resistance. The optimal parameters for achieving the maximum strength were a welding current of 200 A, gas flow rate of 10 L/min, and welding rate of 58 mm/s. The study of ANOVA reveals that the strength of the material in an AA6061 TIG weld is significantly influenced by the rate at which gas flows.

A recent advancement in TIG welding, in which a combination of gases is used as the shielding gas, has occurred[12]. This allows for a higher concentration of energy per unit area during the TIG welding. This technique employs a dual-layer shielding gas in combination with pure Ar. Increasing the viscosity of an arc weld can enhance its energy density by introducing active (such as oxygen and hydrogen) or inert gases (such as helium). A study examined the tensile strength of TIG welding in low-carbon steel. This study utilized St 37 double V joints[13]. The results indicated that TIG welding with a V-double connection demonstrated an average tensile stress of 552.62 N/mm². Prior research has

analyzed and explored the application of TIG welding using SUS 316 L and different carbon steel materials[14]. The research included additional input variables, namely, ER316L and ER70S fillers. The chosen variables for the examination were the microstructure, hardness, and tensile strength. This study indicates that the ER70S filler exhibits a higher tensile strength than the ER70 filler. ER316L and ER70S fillers achieved tensile strengths of 410 MPa and 405 MPa, respectively.

Prior studies have thoroughly examined TIG welding. Nevertheless, the literature suggests that further investigation is required to enhance the effectiveness of TIG welding variables on the dynamic tensile load of low-carbon steels of different thicknesses. This study investigated the impact of input variables

on the Tungsten Inert Gas (TIG) welding process of thin, variable-thickness, low-carbon steel materials. The Taguchi method of experimentation, employing a three-level design and three input variables, was selected to investigate the effects of TIG welding factors. The input parameters included the electrode dimensions, weld current magnitude, and gas flow rate. This study aims to produce significant and valuable knowledge regarding the welding process used for thin plates that are frequently encountered in automotive body repair. The findings are substantial, expected, and enhanced to offer valuable insights for small and medium-sized businesses involved in various automotive body repair establishments.

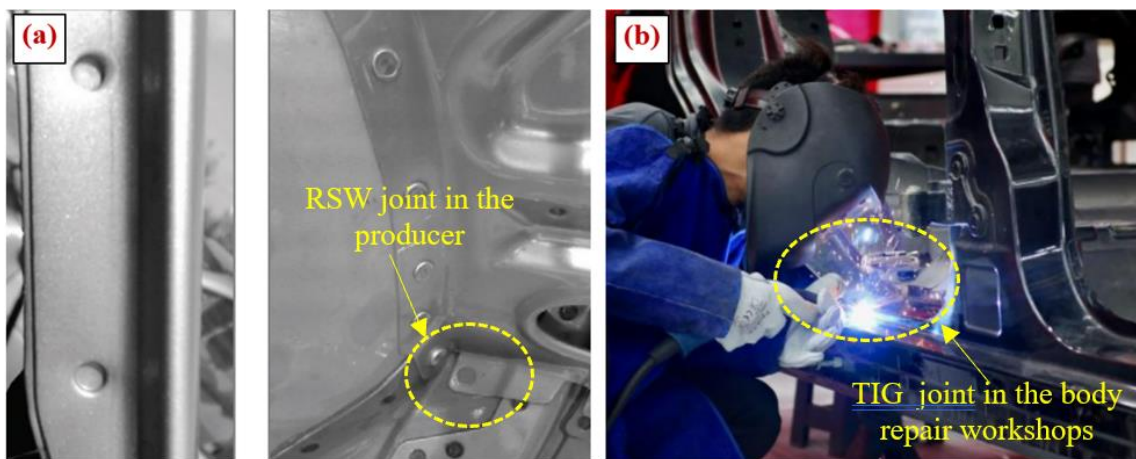


Fig. 1. Thinning material and body repair. (a) The interior and side of the hood. The side part of the hood and the inside of the car[4], (b) the welding process on the interior of the vehicle[5].

2 Methods

The process of conducting TIG welding using the Taguchi method can be divided into several stages. This study employed the Taguchi method to optimize the procedure by identifying the crucial factors and controlling their conditions. Fig. 2 depicts a flowchart outlining the investigation conducted in this study.

2.1 Material

The primary reason for selecting low-carbon steel with thicknesses of 0.6 and 0.8 is its widespread use as the main steel material in automobile bodies and its easy availability in the market. This determination followed the guidelines specified in EN 10111:2008 and EN 10142:2000 regarding the use of sheet steel in automotive body parts. Table 1 presents a comprehensive collection of material suggestions for the automotive body components. The elemental compositions and underlying mechanical characteristics of the materials are presented in Table 2. During the welding process, the elemental composition of the primary metal is a critical parameter. It is crucial to select a

welding filler whose chemical composition closely resembles that of the base metal. The chemical compositions and mechanical properties of the low-carbon steels used in this study are listed in Table 2.

This investigation utilized the TIG ER70S-6 material as a filler rod, which conforms to the AWS A5.18/ASME SFA5 classified standard in the TIG welding process. PT Denki manufactured the welding filler ER70S-6 with diameters of 1.6, 2.0, and 2.4 mm to match the chemical composition of the intended material. In addition, the ER70S-6 filler demonstrated better mechanical characteristics than the bonded material and adhered to the guidelines outlined in the ASME specifications[15]. The upper limits for the chemical compositions of C, Mn, Si, P, and S on the electrode were 0.06%–0.15%, 1.40%–1.85%, 0.025%, and 0.035%, respectively[16]. Simultaneously, the mechanical properties required a minimum of 480 N/mm², 400 N/mm², and 22% elongation for tensile strength, yield strength, and elongation, respectively[17].

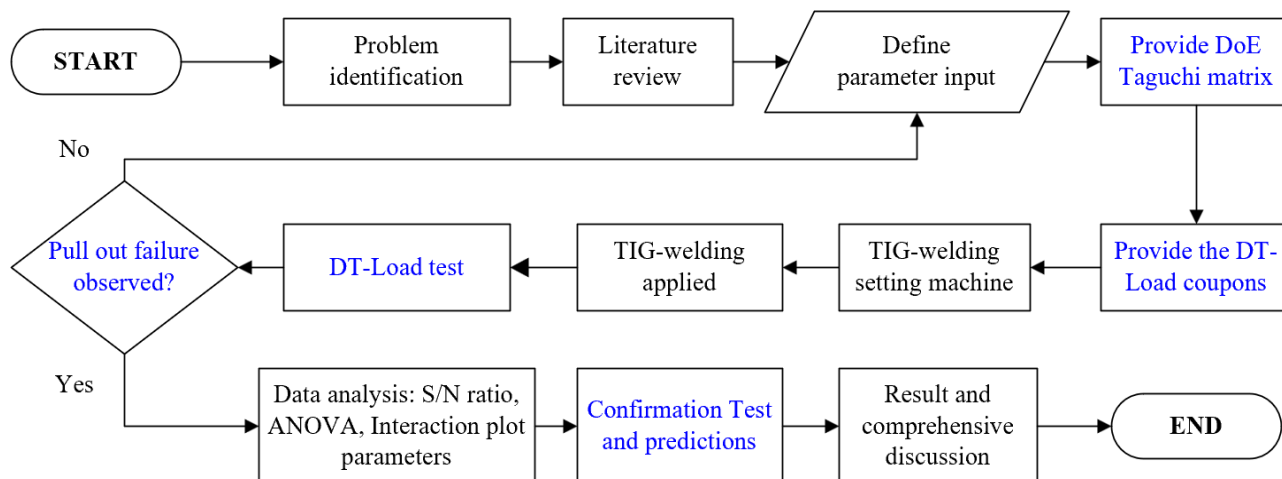


Fig. 2. The Taguchi optimization of TIG welding flowchart.

Table 1. Mechanical properties of steel sheet for automobile body component[6]

Specification	Material DD13*		Material DD14*				Material DX53D+Z**
	1	2	1	2	3	4	1
Thickness (mm)	0.70	0.80	0.62	0.70	0.80	0.90	0.98
Yield strength (N/mm ²)	179.0	193.0	153.0	162.0	167.0	175.0	239.0
Tensile strength (N/mm ²)	315.0	324.0	270.0	279.0	281.0	285.0	341.0
Elongations (%)	44.0	41.0	46.0	42.0	44.0	42.0	36.0

2.2 Design and Testing of TIG-Welded Joints

This study aimed to determine the welding joint type to achieve the highest possible DT-load. Therefore, the most suitable joint is the butt joint complemented by a backing plate. However, the tapping plate attachment must adhere to established criteria. The JIS G3141 standard was specified using a plate made of low-carbon steel, which was accurately cut according to the procedure illustrated in Fig. 2. As per the procedure outlined above, a hole with a diameter of 10.0 mm was drilled into the backing plate to serve as a filler. The DT-load was measured using a Shimadzu AGS-X 10kN STD E200V Universal Testing Machine at a velocity of 35 mm/min.

The variable load was used as the dependent variable. Fig. 3(a) shows the organization and uniformity of the tensile testing devices used to measure the force in Newtons (N). The connection pattern employed in this study is depicted in Fig. 3(b).

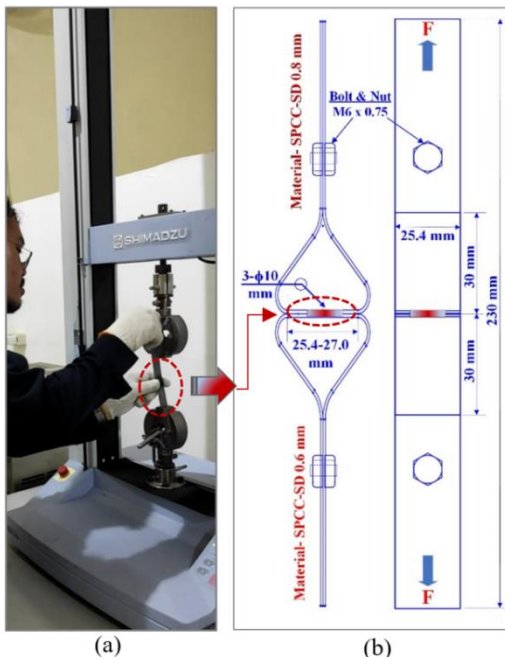


Fig. 3. TIG welding. (a) DT-load test and (b) coupon design.

Taguchi's design for experiments has found wide use in many welding contexts, including resistance spot welding [1, 18, 19], SMAW [20], and GTAW [21]. Moreover, optimising operations in the textile industry [22], painting [23], and machining [24] makes effective use of this method. To determine the optimal TIG welding input factor for DT-load optimisation for various

materials, the thickness of steel with low carbon content, the Taguchi experimental approach was chosen based on previous research. Table 2 lists the Taguchi design factors used in this study. This study examines three control variables at three levels. The three variables under control generated six degrees of freedom.

Table 2. TIG welding process parameters and their varying values

Level	A-Gas flow rate, v	B-Welding current I ,	C-Diameter
	(A) LPMs	Ampere	electrode, d mm
1	10.0	50.0	1.60
2	12.0	55.0	2.00
3	15.0	60.0	2.40

The Daiden TIG 200 welding circuit, shown in Fig. 4, was chosen to prepare the DT-load coupon. Argon gas with a purity of approximately 99.9% was used for TIG welding, and the welding current range was limited to 10–200 s, while the input voltage and frequency were set at 220 V/50 Hz. Welders with a minimum 5G licence are mandated to adhere to safety regulations while performing the welding procedure at position 1G. The input variables were determined to be the argon gas flow rate, the tungsten electrodes' size, and the electric current. Furthermore, the DT-load was selected for simultaneous comprehensive evaluation. The 18 coupons used in the DT-load test were executed twice for each run, as depicted in Fig. 5. This was performed to assess the consistency of the data.



Fig. 4. TIG welding preparations.

mm-thick SPCC-SD steel measuring 0.6 and 0.8 mm thick was chosen for sample preparation in the DT-load tests. The constituent elements and material characteristics of SPCC-SD steel are listed in Table 3.



Fig. 5. 18-unit sample TIG welding using different thickness low carbon steel.

Table 3. The chemical composition and mechanical properties of low-carbon steel sheet material

Specification	Mechanical properties			Chemical composition (%)			
	YP (N/mm ²)	TS (N/mm ²)	EL (%)	C	Mn	P	S
JIS G 3141	≤ 240.0	≥ 270.0	≥ 37.0	≤ 0.150	≤ 0.600	≤ 0.040	≤ 0.050
Coil-SP51023 (0.6 mm)	195.0	315.0	44.0	0.03640	0.1920	0.0100	0.00500
Coil-SP51023 (0.8 mm)	195.0	315.0	44.0	0.03640	0.1920	0.0100	0.00500

2.3 Signal to Noise Ratio (S/N Ratio)

The S-N ratio is the most precise method for determining the optimal value of a variable output [25]. The signal-to-noise (S/N) ratio was determined by computing the average quality attributes of the output. The Taguchi approach provides multiple viable options, including size-by-size, nominal, and larger, to determine the quality of the final result data. Eq. 1 – Eq. 3 denote a group of equations that is equal to each output characteristic[25, 26].

Larger is better:

$$S - N \text{ ratio} = -10 \log \frac{1}{n_0} \sum_{i=1}^{n_0} \frac{1}{y_i^2} \quad (1)$$

Smaller is better:

$$S - N \text{ ratio} = -10 \log \sum_{i=1}^{n_0} \frac{y_i^2}{n_0} \quad (2)$$

Nominal is the best:

$$S - N \text{ ratio} = -10 \log \frac{\bar{y}^2}{s^2} \quad (3)$$

Where n represents the number of samples, y represents the response factor, \bar{y} represents the average of response factors, and s represents the variance of response factors.

This study utilized randomized selection to conduct nine Orthogonal Array (OA) trials. The TIG welding parameters were meticulously calibrated for each proficiency level, considering the values specified in Table 2. Two responses were recorded for each configuration. Table 4 displays the mean DT-load and S-N ratio. Eq. 1 quantifies the signal-to-noise ratio as a performance measure, with a higher value indicating a higher DT-load. The findings of this study substantiated and verified the reports in [21, 27]. Regression modeling was employed to precisely forecast the impact of the input variables on the S-N ratio.

3 Results and Discussion

3.1 Direct Tensile Load (DT-Load) Analysis

DT-load results are essential for understanding how welding parameters affect the durability of welded joints. DT-load measurements vary significantly in the table. Run No. 6 had the highest DT-load at 4410.0 N with a gas flow rate of 12.0 LPM, welding current of 60.0 A, and electrode diameter of 1.60 mm, as shown in Fig. 6(a). With a gas flow rate of 10.0 LPM, a welding current of 50.0 A, and the same electrode diameter, Run No. 1 had

the lowest DT-load of 2229.5 N. The table shows large DT-load differences. Run No. 6 had the highest DT-load at 4410.0 N with a gas flow rate of 12.0 LPM, welding current of 60.0 A, and electrode diameter of 1.60 mm. With a gas flow rate of 10.0 LPM, a welding current of 50.0 A, and the same electrode diameter, Run No. 1 had the lowest DT-load of 2229.5 N. This comparison shows how welding parameters, such as the gas flow rate and welding current, affect joint strength.

Further analysis optimised these variables to strengthen the welded joint. The specific parameter combination in Run No. 1 caused the weakest joint strength, demonstrating the importance of welding parameters in determining vulnerability. This emphasises the importance of fine-tuning parameters to strengthen the welded joints.

3.2 TIG Welded Visual Examination

The DT-load test is an essential method for analyzing the dynamics of welding joint failures. To comprehend DT-load, one must classify the outcomes of tensile tests for TIG welding into two main categories of failure: "interface failure" and "pull-out failure", as described in reference [35]. Interface failure is commonly caused by insufficient fusion of the filler during welding, frequently resulting from an inadequate TIG welding current. The consequence is a less robust joint than the welded material, distinguished by a non-penetrating bead produced by the low welding current, which complicates the weld initiation and has an uneven arc. In contrast, pull-out failure manifests itself when the strength of the welded material is exceeded by a joint welded using TIG welding[1, 28]. This phenomenon is frequently observed in various welding applications, including TIG welding. A pull-out failure mode was consistently observed upon visual inspection of TIG-welded specimens that underwent DT-load testing. This finding suggests that the fusion between the filler and mild sheet steel is robust, spanning all parameters. The pull-out failure mode of the TIG-welded low-carbon steel sheet joints is illustrated in Fig. 6(b).

The Heat-Affected Zone (HAZ) is where pull-out failure occurs, as shown in Fig. 5. This failure is caused by a reduced DT-load caused by heat exposure during the TIG welding process [9]. The successful fusion of materials has enabled the efficient application of electric currents in TIG welding[29, 30]. Table 4 presents the results indicating that the sixth iteration yielded the highest DT-load of 3457.13 N when particular TIG welding parameters were employed: a flow rate of 10 L/min, a welding current of 60 A, and an electrode diameter of 1.6 mm. A graphical representation of the maximum DT-load test resulting from these conditions is shown in Fig. 6.



Fig. 6. The load of TIG welding. (a) The highest DT-load chart as recommended by the Taguchi experiment, and (b) pull-out failure mode.

Table 4. Experimental data for DT-load and S-N ratio

Run No.	Gas Flow rate	Weld. current	Electrode diameter	DT-load (N)			S-N ratio	
				R-1	R-2	Mean	Exp.*	Pred.*
1	10.0	50.0	1.60	2229.5	1557.6	1893.54	65.13	65.86
2	10.0	55.0	2.00	2561.6	2695.1	2628.33	68.39	68.25
3	10.0	60.0	2.40	3415.0	3133.5	3274.22	70.28	70.64
3	12.0	50.0	2.00	2841.9	2811.1	2826.49	69.02	68.19
5	12.0	55.0	2.40	3272.8	3415.3	3344.02	70.48	70.58
6	12.0	60.0	1.60	4410.0	3621.1	4015.56	71.95	70.74
7	15.0	50.0	2.00	3320.9	3592.9	3456.93	70.75	70.51
8	15.0	55.0	2.40	3229.0	3085.5	3157.23	69.98	70.68
9	15.0	60.0	1.60	4304.1	4199.1	4251.61	72.57	73.07

Note: Gas flow rate in L/ minutes, weld. Current A, Electrode diameter (mm), Exp.= experimental, Pred.= predicted.

3.3 S-N Ratio analysis

The S-N ratio evaluation aims to assess the effects of varying input factor concentrations [28]. To calculate and ascertain the average S-N ratio, the average S-N ratios at Levels 1, 2, and 3 were obtained (Fig. 7). The effect is substantial, as the values of the parameters that differ significantly affect the response. The S/N ratios for every TIG welding procedure variable, including both the experimental and predicted DT-loads, are presented in Table 4.

By examining the response information for the input parameters, this analysis forecasts the most suitable parameter values using linear multiple regression. The results of a regression study conducted using statistical tools were computed using Eq. 4.

$$S - N \text{ Ratio}_{\text{predict.}} = 38.50 + 0.792A + 0.3295B + 1.854C(4)$$

Where A argon gas flow rate, B is the welding current, and C is the electrode diameter.

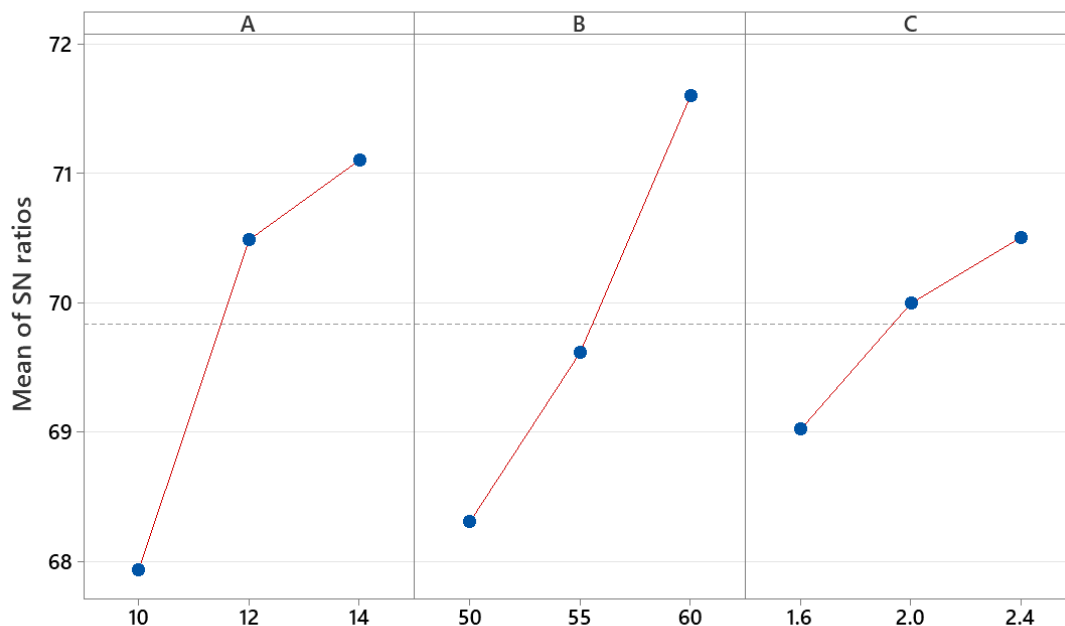
The use of multiple regression linear analysis to forecast outcomes from scientific data is supported by prior research, which provides additional evidence for this methodology [4, 19, 27]. The present investigation employed regression analysis to forecast the S-N ratio; the results are presented in Table 5. Upon comparison and calculation with experimental data, the T-S prediction demonstrated an average level of precision of approximately 7%. This was a noteworthy achievement. The accuracy of this result surpasses those of the rates of 13.92% [31] and 10% [32], which were previously examined.

The S-N ratio response Table 5 demonstrates the impact of three factors, namely flow rate, welding current, and electrode diameter, on the "larger is better" characteristic in the DT-load of the TIG welding process. According to the ranking analysis, the welding current factor (B) had the highest level of influence, ranking first. Subsequently, the flow rate factor (A) was ranked second, whereas the electrode diameter (C) was ranked third. These findings emphasize that modifying the welding current significantly enhanced the S-N ratio under DT-loads. The primary emphasis in enhancing the desired outcomes in TIG welding is on this factor, with flow rate regulation being of secondary importance. Simultaneously, the electrode diameter appears to have less influence on this characteristic. The examination of this table offers valuable insights for selecting the optimal parameters to enhance the signal-to-noise ratio in TIG welding processes concerning DT-load.

Table 5. Response table for the S-N ratio of the "larger is better" characteristic on DT-load of TIG welding

Level	Flow rate, v (A)	Welding current I , (B)	Diameter electrode, d (C)
1	67.93	68.3	69.02
2	70.48	69.61	69.99
3	71.1	71.6	70.5
Delta	3.17	3.29	1.48
Rank	2	1	3

Main Effects Plot for SN ratios
Data Means



Signal-to-noise: Larger is better

Fig. 7. S-N Ratio larger is better graph for D-T strength of TIG welding.

3.4 Analysis of Variance (ANOVA)

ANOVA was used to ascertain the design factors that significantly impacted the output variable, with a confidence level of 95% in establishing statistical significance. As observed in [34], the percentage contribution of each factor indicates the amount of reduction in variation explained. It is worth noting that even a minimal deviation in a parameter representing a significant percentage contribution can substantially impact performance. The ANOVA result analysis listed in Table 6.

The ANOVA results indicate that factors A (flow rate) and B (welding current) have significant F-values and low P-values. Specifically, factor B has an F-value of 15.86 with a P-value of 0.059, while factor A has an F-value of 13.71 with a P-value of 0.068. This suggests that variations in the flow rate and welding current can lead to substantial differences in DT-load. Factor C, which represents the electrode diameter, had a lower F-value and a higher P-value (1.37 with a P-value of 0.421). Factor C may have a minor impact on the variation in DT-load. The welding current

(B) factor had the highest contribution of 51.25%, followed by the flow rate (A), which contributed 44.30%. The contribution of electrode diameter (C) was only 4.44%. Within this particular framework, the primary emphasis in enhancing or regulating the DT-load in TIG welding procedures may lie in modifying the flow rate and welding current. This means that these factors substantially influenced the fluctuations observed in the DT-load outcomes.

The results of the ANOVA indicate that specific variables, namely welding current and gas flow rate, significantly impact the variation in DT-load. Nevertheless, the impact of the electrode diameter might be relatively insignificant compared to other determinants. The diameter of the electrode does not affect the strength of the connection because the diameter of the electrode is not an essential variable. The diameter of the electrode is related to the current used; the larger the electrode, the greater the current used.

Table 6. ANOVA for DT-load of TIG welding

TIG welding parameters	DOF	Seq SS	Adj MS	F-value	P-value	% Contribution
A-flow rate, v (L/minute)	1732980	1732980	866490	13.71	0.068	44.30%
B-welding current I , (A)	2004857	2004857	1002429	15.86	0.059	51.25%
C-diameter electrode, d (mm)	173712	173712	86856	1.37	0.421	4.44%
Residual error	126443	126443	63221			
Total	4037993					100.0%

3.5 Interaction Plot Parameter Analysis

The means for each categorical variable value are depicted in an interaction plot and matrix diagram, as shown in Fig. 8. The significance of each parameter was evaluated using ANOVA, a statistical technique that calculates confidence levels by measuring data dissimilarity. Analyzing the differences between parameters to determine the levels of certainty, ANOVA does not interpret the data directly. The principal influence of a categorical variable was ascertained through a slope examination. A horizontal line (x-axis parallel) indicates no substantial variation or distinction between tiers in the average response of the factor [32].

A visual representation of the relationship between DT-load and welding current (B) \times electrode diameter (C), flow rate (A) \times welding current (B), and welding current (B) \times electrode diameter (C) is shown in Fig. 7. As evidenced by the parallel and unrelated lines, the contributions of A \times B and A \times C to DT-load exhibit

minor interactions. However, as indicated by the intersection of the lines, the interaction between B and C substantially affects the DT-load [32, 33]. It depicts the interaction plot theory corresponding to these observations.

The interaction plot image reveals that the fluctuations in the DT-load value (direct tensile load) are contingent upon the amalgamation of the input parameters, namely, the gas flow rate, welding current, and electrode diameter. Examination of the correlation between these parameters and mean DT-load revealed various noteworthy patterns. Each row in the table details a particular arrangement of these parameters. Obtainable observations include the impact of the gas flow rate, welding current, and electrode diameter on the DT-load. For instance, when the gas flow rate was set at 10.0 LPM, the average DT-load value increased as the welding current was raised from 50.0 A to 60.0 A, using the same diameter electrode (e.g., Run 1-3).

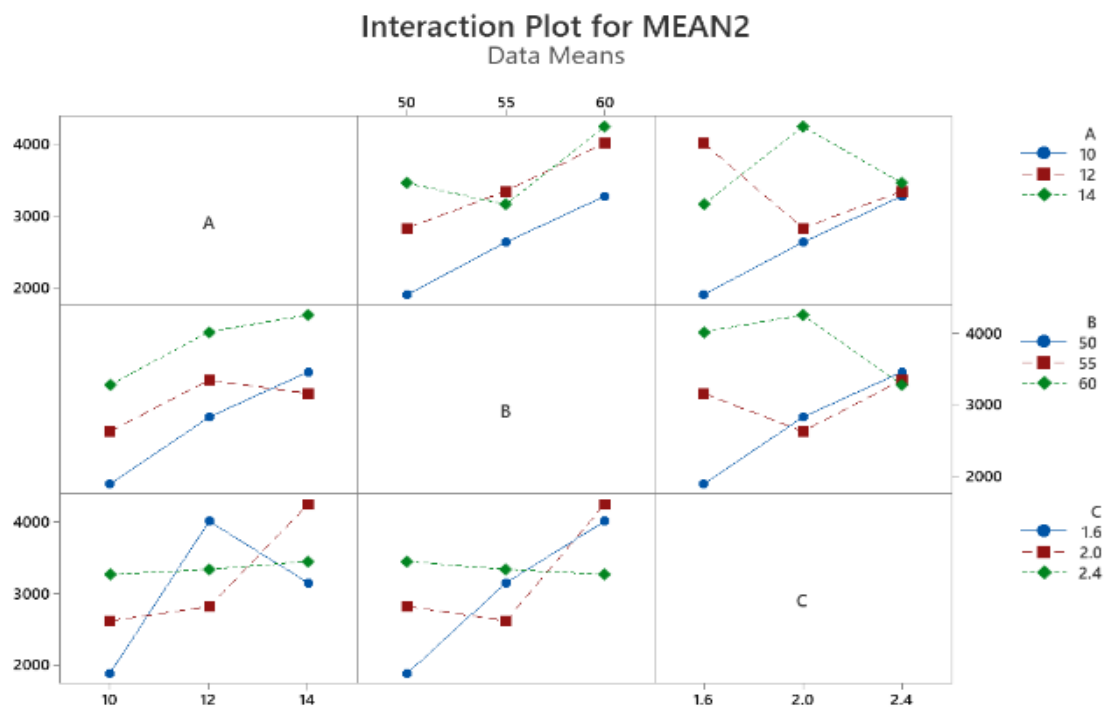


Fig. 8. The interaction plot of each parameter of TIG welding application.

Nevertheless, when the gas flow rate is set at 15.0 LPM, raising the welding current from 50.0 A to 60.0 A does not result in a corresponding rise in the average value of DT-load, as observed in Run 7-9. The impact of welding current was equally substantial. It is evident that when the gas flow rate and electrode diameter remain constant, increasing the welding current value increases the average DT-load (e.g. Runs 3, 6, and 9).

The impact of electrode diameter is also evident, although it may consistently follow different patterns for every combination of parameters.

3.6 Confirmation test parameters

In the last stage of the preliminary iteration of the experimental design process, the confirmation experiment verified the conclusions derived during the analysis phase. This entails scrutinizing a particular amalgamation of parameters and levels that have been previously assessed. Taguchi experiments were

purposefully devised and implemented to determine the most favorable conditions and approximate responses while utilizing the optimal levels of TIG welding parameters. To establish these conditions, TIG welding parameters were generated. Estimation and validation of the performance data enhancement constitutes the final phase. The statistical software estimated the mean S-N ratio and DT-load using multi-linear regression. Eq. 3 was applied to ascertain the anticipated mean S-N ratio. Simultaneously, the DT-load forecast was calculated using Eq. 5.

$$\text{Mean}_{\text{ts,p}} = -6032 + 255A + 112.1B \quad (5)$$

A represents the argon gas flow rate, B represents the current used in TIG welding, and C represents the electrode diameter. The confirmation test results are presented in Table 7.

Table 7. The confirmation experimental results

Description	Initial process	Optimal process parameter		Improvement (%)	
	factors ¹⁾	Predicted	Experimental	Predicted	Experimental
Level	A ₁ ; B ₁ ; C ₁ ;	A ₃ ; B ₃ ; C ₃ ;	A ₂ ; B ₃ ; C ₁ ;		
S-N Ratio	65.13	72.57	73.07	11.4	12.2 %
DT-load average (N/mm ²)	1893.55	4264.00	4251.61	125.2%	124.5%

The confirmation test table illustrates the successful application of the identified process factors, as indicated by the shift from the initial levels A₁, B₁, and C₁ to the optimal levels A₃, B₃, and C₃. This transition results in significant improvements in the measured parameters. The S-N Ratio, or signal-to-noise ratio, shows a substantial increase from the initial forecast of 65.13 to 73.07 in ideal conditions, representing a 12.2% improvement. This shows that improving the process factors dramatically increases the relationship between the signal and noise in the measurement data. Significant progress has been made, particularly when compared with the findings of other researchers[11].

Regarding the DT-load, the results determined the optimal conditions for TIG welding. The spark generated between the electrode and the workpiece causes the object to melt. Imperfections on the surface of the electrode can reduce the size of the Heat-Affected Zone (HAZ) [32]. Moreover, the DT-load average, which indicates the average direct tensile load in N/mm², significantly increased from 1893.55 in the initial prediction to 4251.61 under ideal conditions. The data showed a significant increase of 124.5%, indicating that the optimal parameters significantly improved the resistance to direct tensile loads. To summarise, the confirmatory tests demonstrate that optimising process parameters results in significant improvements in both measured parameters (S-N ratio and DT-load average), thereby confirming the effectiveness of adjusting conditions to achieve optimal outcomes in enhancing the performance or quality of the observed processes.

4 Conclusion

Taguchi optimization in TIG welding with three variables and three levels of experimentation on thin plates has produced noteworthy outcomes. Optimal parameters improve the direct tensile load (DT-load), significantly boosting joint strength and stability. The highest DT-load was achieved at 4410.0 N with a TIG welding parameter of a gas flow rate of 12.0 LPM, welding current of 60.0 A, and electrode diameter of 1.60 mm. The ideal DT-load value increases substantially following optimization, indicating that the welded joint's durability and strength have been significantly enhanced. Assessing process quality involves analyzing the signal-to-noise ratio (S-N ratio), which significantly improves from initial to optimal levels, suggesting enhanced structural integrity and joint quality. ANOVA analysis shows that

welding current and gas flow rate significantly influence DT-load variability, while electrode diameter has minimal impact. Confirmatory tests, ANOVA analysis, determining optimal DT-load values, and improving the S-N ratio highlight the importance of adjusting process parameters to enhance the quality and strength of TIG welding. Exploring the connections between variables offers valuable insights into how different parameter combinations affect the results of a process. These analyses provide valuable information for improving processes and increasing efficiency and effectiveness in TIG welding on thin plates.

Acknowledgement

The research has been fully funded by "BELMAWA" through the "(Program KreativitasMahasiswaRisetEksata 2022) (PKM-RE)". The support rendered by the mechanical engineering laboratory staff of UBP Karawang and the automotive repair shop "WaroenkBodykit" was highly valued while gathering data. The support rendered by the mechanical engineering laboratory staff of UBP Karawang and the automotive repair shop "WaroenkBodykit" was highly valued while gathering data.

References

- [1] S. Sukarman, A. Abdulah, A. D. Shieddieque, N. Rahdiana, and K. Khoirudin, "OPTIMIZATION OF THE RESISTANCE SPOT WELDING PROCESS OF SECC-AF AND SGCC GALVANIZED STEEL SHEET USING THE TAGUCHI METHOD," *SINERGI*, vol. 25, no. 3, pp. 319-328, 2021.
- [2] D. L. Parker, A. Bejan, and L. M. Brosseau, "A qualitative evaluation of owner and worker health and safety beliefs in small auto collision repair shops," *American Journal of Industrial Medicine*, vol. 55, no. 5, pp. 474-482, 2012.
- [3] Raincatcher, "AUTO BODY Table of Contents," 2022, Available: https://raincatcher.com/images/raincatcher_images/auto-body-shops-auc.pdf.
- [4] J. Mucha, L. KašČÁK, and E. SpiŠÁK, "Joining the car-body sheets using clinching process with various thickness and mechanical property arrangements," *Archives of Civil and Mechanical Engineering*, vol. 11, no. 1, pp. 135-148, 2011.

- [5] A. Arfian. (2022, 9 January). *6 Bengkel Body & Paint Mercedes-Benz Kini Tersertifikasi Jerman*. Available: <https://cintamobil.com/perawatan-dan-service/6-bengkel-body-paint-mercedesbenz-kini-tersertifikasi-jerman-aid20232>
- [6] E. Budiyanto, E. Nugroho, and A. Masruri, "Pengaruh Diameter Filler Dan Arus Pada Pengelasan Tig Terhadap Kekuatan Tarik Dan Struktur Mikro Pada Baja Karbon Rendah," *Teknik Mesin Univ. Muhammadiyah Metro*, vol. 6, no. 1, 2017.
- [7] L. Andewi, "Pengaruh Variasi Arus Pada Hasil Pengelasan Tig (Tungsten Inert Gas) Terhadap Sifat Fisis Dan Mekanis Pada Aluminium 6061," Semarang, 2016.
- [8] K. Kobayash *et al.*, "Practical application of high efficiency twin-arc TIG welding method (sedar-TIG) for PCLNG storage tank," *Welding in the World*, vol. 48, no. 7-8, pp. 35-39, 2004.
- [9] S. Tathgir, D. W. Rathod, and A. Batish, "Emphasis of Weld Time, Shielding Gas and Oxygen Content in Activated Fluxes on the Weldment Microstructure," *Mechanical Engineering for Society and Industry*, vol. 1, no. 2, pp. 86-95, 2021.
- [10] F. A. Abdillah, "Pengaruh Variasi Arus Dan Kecepatan Pengelasan Tig Terhadap Struktur Mikro Dan Kekerasan Baja Tahan Karat SS 316L," 2017.
- [11] V. Mohanavel, M. Ravichandran, and S. Suresh Kumar, "Optimization of tungsten inert gas welding parameters to attain maximum impact strength in AA6061 alloy joints using Taguchi Technique," *Materials Today: Proceedings*, vol. 5, no. 11, pp. 25112-25120, 2018.
- [12] Y. Xie, Y. Cai, X. Zhang, and Z. Luo, "Characterization of keyhole gas tungsten arc welded AISI 430 steel and joint performance optimization," *International Journal of Advanced Manufacturing Technology*, vol. 99, no. 1-4, pp. 347-361, 2018.
- [13] B. Anwar, "Analisis Kekuatan Tarik Hasil Pengelasan Tungsten Inert Gas (Tig) Kampuh V Ganda Pada Baja Karbon Rendah St 37," *Teknologi*, vol. 17, no. 3, pp. 33-38, 2018.
- [14] Z. Nurisna and E. Setiawan, "Pengaruh Filler Pada Pengelasan Tig Baja Karbon Dan Stainless Steel 316L Terhadap Sifat Mekanik," *Quantum Teknika : Jurnal Teknik Mesin Terapan*, vol. 1, no. 2, pp. 95-99, 2020.
- [15] D. L. Olson, S. Thomas A, S. Liu, and G. R. Edwards, *Welding, brazing, and soldering*. ASM International, 1990.
- [16] Asme, "ASME Boiler and Pressure Vessel Code, Section II Part C - Specifications for Welding Rods, Electrodes, and Filler Metals," "Specification for titanium and titanium-alloy welding electrodes and rods," ed, 2010, pp. 377-390.
- [17] A. A. M. Aws, "AWSA5.18-A5.18M-2005.pdf," ed, 2005.
- [18] S. Sukarman and A. Abdulah, "Optimasi parameter resistance spot welding pada pengabungan baja electrogalvanized menggunakan metode Taguchi," *Dinamika Teknik Mesin*, vol. 11, no. 1, pp. 39-48, 2021.
- [19] F. Mucharom *et al.*, "Tensile shear load in resistance spot welding of dissimilar metals: An optimization study using response surface methodology," *Mechanical Engineering for Society and Industry*, vol. 3, no. 2, pp. 66-77, 2023.
- [20] K. E. K. Vimal, S. Vinodh, and A. Raja, "Optimization of process parameters of SMAW process using NN-FGRA from the sustainability view point," *Journal of Intelligent Manufacturing*, vol. 28, no. 6, pp. 1459-1480, 2017.
- [21] R. S. Vidyarthi and D. K. Dwivedi, "Activating flux tungsten inert gas welding for enhanced weld penetration," *Journal of Manufacturing Processes*, vol. 22, pp. 211-228, 2016.
- [22] A. Budianto, S. Sukarman, S. B. Jumawan, and A. Abdulah, "OPTIMASI RESPON TUNGGAL PADA PROSES TEXTURING BENANG DTY-150D / 96F MENGGUNAKAN METODE TAGUCHI SINGLE RESPONSE OPTIMIZATION OF DTY-150D / 96F YARN TEXTURING PROCESS USING TAGUCHI METHOD," *Arena Tekstil*, vol. 35, no. 2, pp. 77-86, 2020.
- [23] S. Sukarman, A. D. Shieddieque, C. Anwar, N. Rahdiana, and A. I. Ramadhan, "Optimization of Powder Coating Process Parameters in Mild Steel (Spcc-Sd) To Improve Dry Film Thickness," *Journal of Applied Engineering Science*, vol. 19, no. 2, pp. 1-9, 2021.
- [24] K. Khoirudin, S. Sukarman, N. Rahdiana, A. Suhara, and A. Fauzi, "Optimization of S-EDM Process Parameters on Material Removal Rate Using Copper Electrodes," *Jurnal Polimesin*, vol. 21, no. 1, pp. 17-20, 2023.
- [25] S. Sukarman *et al.*, "OPTIMAL TENSILE-SHEAR STRENGTH OF GALVANIZED/MILD STEEL (SPCC-SD) DISSIMILAR RESISTANCE SPOT WELDING USING TAGUCHI DOE," *Jurnal Teknologi*, vol. 4, pp. 167-177, 2023.
- [26] P. G. Mathews, *Design of Experiments with MINITAB*, 12 ed. Milwaukee: Mathews, Paul G., 2005, pp. 205-205.
- [27] X. Wan, Y. Wang, and D. Zhao, "Multi-response optimization in small scale resistance spot welding of titanium alloy by principal component analysis and genetic algorithm," *International Journal of Advanced Manufacturing Technology*, vol. 83, no. 1-4, pp. 545-559, 2016.
- [28] Y. G. Kim, D. C. Kim, and S. M. Joo, "Evaluation of tensile shear strength for dissimilar spot welds of Al-Si-Mg aluminum alloy and galvanized steel by delta-spot welding process," *Journal of Mechanical Science and Technology*, vol. 33, no. 11, pp. 5399-5405, 2019.
- [29] G. Venkatesan, V. Muthupandi, and J. Justine, "Activated TIG welding of AISI 304L using mono- and tri-component fluxes," *International Journal of Advanced Manufacturing Technology*, vol. 93, no. 1-4, pp. 329-336, 2017.
- [30] B. Xing, Y. Xiao, Q. H. Qin, and H. Cui, "Quality assessment of resistance spot welding process based on dynamic resistance signal and random forest based," *International Journal of Advanced Manufacturing Technology*, vol. 94, no. 1-4, pp. 327-339, 2018.
- [31] N. K. Singh and Y. Vijayakumar, "Application of Taguchi method for optimization of resistance spot welding of austenitic stainless steel AISI 301L," *Innovative Systems Design and Engineering*, vol. 3, no. 10, pp. 49-61, 2012.
- [32] H. Wu, Y. Chang, Q. Mei, and D. Liu, "Research advances in high-energy TIG arc welding," *International Journal of Advanced Manufacturing Technology*, vol. 104, no. 1-4, pp. 391-410, 2019.
- [33] X. Ding, H. Li, L. Yang, Y. Gao, and H. Wei, "Numerical analysis of arc characteristics in two-electrode GTAW," *International Journal of Advanced Manufacturing Technology*, vol. 70, no. 9-12, pp. 1867-1874, 2014.